Materials Science in Semiconductor Processing 172 (2024) 108040

Contents lists available at ScienceDirect

Materials Science in Semiconductor Processing

journal homepage: www.elsevier.com/locate/mssp

Synthesis and properties of β-Ga_2O_3 nanowires and nanosheets on doped GaS:Mn substrates

Veaceslav Sprincean [a], Haoyi Qiu [b], Oleg Lupan [b,c,d,*], Tim Tjardts [e], Deik Petersen [b], Salih Veziroglu [e], Rainer Adelung [b], Mihail Caraman [a]

[a] Faculty of Physics and Engineering, Moldova State University, 60 Alexei Mateevici str., MD-2009, Chisinau, Republic of Moldova
[b] Functional Nanomaterials, Faculty of Engineering, Institute for Materials Science, Kiel University, Kaiserstr, 2, D-24143, Kiel, Germany
[c] Center for Nanotechnology and Nanosensors, Department of Microelectronics and Biomedical Engineering, Technical University of Moldova, 168, Stefan cel Mare Av., MD-2004, Chisinau, Republic of Moldova
[d] Department of Physics, University of Central Florida, Orlando, FL, 32816-2385, USA
[e] Chair for Multicomponent Materials, Institute for Materials Science, Kiel University, Kaiserstr, 2, D-24143, Kiel, Germany

ARTICLE INFO

Keywords:
Gallium oxide
Gallium sulfide
Manganese
Nanowires
Nanosheets
Doping

ABSTRACT

In this work, the synthesis, morphology, optical and luminescence properties of Mn-doped β-Ga_2O_3 (Ga_2O_3:Mn) nanowires/nanosheets on Mn-doped GaS (GaS:Mn) substrate are studied. The aim was to obtain structures of semiconductors with layers of nanoformations (nanowires, nanosheets) from a wide energy band semiconductor such as β-Ga_2O_3 and to determine their characteristic properties. For the base material, Mn-doped GaS lamellae were chosen, which are optically transparent in the spectral region where the optical properties of Mn^{2+} and Mn^{3+} ions are manifested. Through thermal annealing, single-crystalline β-GaS plates doped with 1.3 atomic percent (at.%) of manganese (Mn) are exposed to an atmosphere enriched with H_2O vapor at a temperature of 800 °C for 6 h. As a result, the surface of these plates is covered with a composite layer consisting of crystallites of α-Ga_2S_3:Mn and β-GaS:Mn planar junctions. This composite exhibits a direct band gap of 2.88 eV and an indirect band gap of 2.55 eV corresponding to the β-GaS:Mn crystallites. Upon further increasing the temperature during thermal annealing to 850 °C and 920 °C, the surface of the β-GaS:Mn samples transform into a layer of β-Ga_2O_3:Mn nanowires/nanosheets with a band gap of 4.5 eV. Its intense green-orange photoluminescence is caused by electronic transitions within the Mn^{2+} ion.

1. Introduction

In recent years, wide bandgap semiconductors have received considerable research attention due to their unique physical properties and potential applications in various electronic devices [1]. Among these semiconductors, compounds such as GaN, $Al_xGa_{1-x}N$, and oxide semiconductors like TiO_2, ZnO, $MgZn_{1-x}O$, and Ga_2O_3 (especially monoclinic β-Ga_2O_3) have attracted particular interest due to their application in ultraviolet radiation photo-detectors (UVB and UVC), power electronic devices, and of UV radiation sources [2–5]. The range of applications of these materials is expanding with the transition from massive bulk single crystals to micro- and nano-crystallites [6,7]. Gallium oxide (β-Ga_2O_3) is a *n*-type semiconductor with a direct bandgap of about 4.4–4.9 eV and a monoclinic crystal lattice. The high-temperature stability of β-Ga_2O_3 can be achieved by doping with chemical elements such as Zn and Sn [8,9]. As a result, it is considered a promising material for use in UV optoelectronics, acting as a photocatalyst for the decomposition of organic pollutants and water, and functioning as a sensor for toxic gases at high temperatures [10–12].

One of the basic parameters that determine the applicability of this material in electronic devices is the critical (breakdown) electric field. For undoped β-Ga_2O_3, the critical electric field is about 8 MV/cm, while for β-Ga_2O_3 doped with Zn, this parameter reaches the value of 13.2 MV/cm. In addition, β-Ga_2O_3:Zn in nanosheets exhibits intense photoluminescence in the green region [13] and shows high sensitivity as a photo-detector in the UVC region, with response reaching up to 210 A/W at a wavelength of 232 nm [14].

Nanostructured undoped and doped β-Ga_2O_3 grown on substrates such as Si, GaN, GaAs, Al_2O_3, and other oxide semiconductors such as TiO_2 and ZnO play an important role in the development of electronic

* Corresponding author. Functional Nanomaterials, Faculty of Engineering, Institute for Materials Science, Kiel University, Kaiserstr, 2, D-24143, Kiel, Germany.
E-mail address: ollu@tf.uni-kiel.de (O. Lupan).

https://doi.org/10.1016/j.mssp.2023.108040
Received 4 July 2023; Received in revised form 18 November 2023; Accepted 3 December 2023
Available online 21 December 2023
1369-8001/© 2023 The Authors. Published by Elsevier Ltd. This is an open access article under the CC BY-NC-ND license (http://creativecommons.org/licenses/by-nc-nd/4.0/).

devices, UV radiation receivers and sources, gas sensors, and photocatalysts [14–17]. It has been shown that the manganese (Mn) dopant induces impurity bands near the band edge, resulting in the decrease of the band gap of the Ga_2O_3 [18].

Considering that GaS:Mn is an optically transparent material in the region where the luminescent transitions of Mn^{2+} and Mn^{3+} ions are manifested, thus also obtaining intense luminescence in the green-orange region. A thorough knowledge of the basic structural, optical and vibrational properties of Mn-doped β-Ga_2O_3/GaS:Mn is crucial, since information on cost-efficient and simple technological approaches and structure is still lacking. Mn - doped composites as β-Ga_2O_3/GaS:Mn are extremely important for fundamental research, as well as for developing new devices, e.g. various applications including optoelectronic sensors, non-toxic biomedical imaging, energy down-conversion in nanostructured solar cells, nonlinear optical applications, optoelectronic devices, e.g., high-power laser radiation sensors. Recent structures demonstrate that Mn-doped β-Ga_2O_3 thin films as well as nanostructured layers are promising materials in light sources in the visible region of the spectrum under electron beam excitation and photon excitation in the UV region.

In this work, the synthesis and morphology of Mn-doped β-Ga_2O_3 (Ga_2O_3:Mn) nanowires/nanosheets on Mn-doped GaS (GaS:Mn) substrates are investigated. Furthermore, the composition as well as the optical and luminescence properties of Mn-doped β-Ga_2O_3 nanowires/nanosheets on a GaS:Mn substrate are investigated in detail.

2. Materials and methods

The layers consisting of β-Ga_2O_3 nanowires/nanosheets doped with Mn on a GaS:Mn substrate were obtained by thermal annealing of plane-parallel plates of GaS single crystals doped with 1.3 at% Mn in air enriched with H_2O vapor. GaS:Mn plates with thicknesses ranging from 0.03 mm to 0.45 mm were annealed in a tubular furnace at temperatures ranging from 800 to 920 °C, and durations ranging from 30 min to 6 h. During the thermal annealing, a flow of air with a relative humidity of ~80 % passed through the furnace tube. As can be seen from the XRD diffractograms, the GaS:Mn sheets with a thickness of 0.03 mm–0.1 mm are transformed into homogeneous layers of β-Ga_2O_3:Mn after 6 h of thermal annealing at a temperature of 920 °C. The thickness of the β-Ga_2O_3:Mn layer on the GaS:Mn substrate can be controlled by varying the duration of thermal annealing. Slabs of GaS doped with 1.3 % Mn were obtained by cleaving single crystals along the (0 0 0 1) plane of β-Ga_2O_3:Mn single crystals with the hexagonal crystal lattice. The quality and parallelism of the surfaces of the GaS:Mn plates were checked by the homogeneity of the interference pattern of a parallel beam of laser radiation at a wavelength of 532 nm. GaS:Mn single crystals were grown by the Bridgman method in a furnace with two temperature ranges. 20 g of the compound could be synthesized from the elemental components Ga(5 N), S(5 N) and Mn(4 N) considered in stoichiometric ratios.

The crystal structure of GaS:Mn ingots and β-Ga_2O_3:Mn nanowire/nanosheet layers was analyzed using wavelength monochromatized XRD patterns. $\lambda_{CuK\alpha} = 1.54060$ Å at 40 kV and 40 mA was used for the XRD, which was performed on a Seifert 3000 TT instrument in the range of 2θ angles ranging from 20° to 90°. The surface morphology of β-Ga_2O_3:Mn nanowires/nanosheets as well as the medial dimensions of the nanoformations were determined by SEM (Carl Zeiss AG, Oberkochen, Germany) at a voltage of 7 kV and a current of 8 μA.

XPS (Omicron Nano-Technology GmbH, Al-anode, 300W) was used to verify the elemental composition of the β-Ga_2O_3 layers and the Mn content formed on the GaS:Mn surface. The charge correction was performed with the C 1s line of carbon at 284.8 eV. The XPS spectra were analyzed using the CasaXPS software (version 2.3.23).

The chemical composition of the primary material GaS and the nanostructured β-Ga_2O_3:Mn layer was identified from Raman spectra recorded with a Micro-Raman spectrometer (Witec Alpha 300 Ra, Ulm, Germany) under laser excitation arc at a wavelength of 532 nm.

The absorption band edge of the β-Ga_2O_3:Mn layer was studied by diffuse reflectance spectra using a Specord M − 40 spectrophotometer complete with an integrated sphere. A layer of $BaSO_4$ was used as a diffuse reflectance standard.

The photoluminescence of the β-GaS:Mn single crystal and the β-Ga_2O_3:Mn nanoformations was recorded in a MDR-type monochromator setup equipped with 600 mm^{-1} and 1200 mm^{-1} diffraction gratings. Photoluminescence (PL) spectra were recorded using a (Na_2K)Sb + Cs photocathode photomultiplier with photosensitivity in the 200–900 nm wavelength range. The PL of the β-GaS:Mn single crystals was excited with 405 nm laser radiation, the PL of the β-Ga_2O_3:Mn layer was excited with 248 nm and 254 nm radiation selected from the arc emission spectrum in Hg vapor (PRK-350 W lamp).

3. Results and discussion

3.1. Morphological studies by scanning electron microscopy (SEM)

The surface morphology of β-GaS:Mn single crystals and the morphological transformations formed as a result of thermal annealing in an atmosphere enriched with H_2O vapors at a temperatures range of 800 °C–920 °C have been studied under SEM as shown in Fig. 1. Fig. 1a shows a fragment of the cross section of a single crystal plate of β-GaS:Mn. The structure of the lamellae and the perfection of the surface of the primary material can be clearly seen. As a result of thermal annealing at a temperature of 800 °C for 6 h, seeds of β- Ga_2O_3:Mn nano-formations with average sizes of ~(30–70) nm and scattered sectors of nanowires are formed on the (0 0 0 1) surface of the mono-crystalline plate (Fig. 1b). Gallium sulfide is a layered semiconductor formed by packings of planar atoms of the type S-Ga-Ga-S with weak polarization bonds between the packings and strong iono-covalent bonds between the atoms in the spacing of the packing. The valence bonds in the sulfur layer on the surface of the GaS plates are closed, so only the defects or dopant on this surface at the initial stage can serve as centers for the nucleation of β-Ga_2O_3 crystallites. At high temperatures, the emission of S atoms occurs, a process that stimulates oxygen diffusion through sulfur vacancies inside the GaS:Mn layer with the formation of β-Ga_2O_3:Mn crystals. This process determines the granular morphology of the sample surface shown in Fig. 1b.

When the annealing temperature is increased to 850 °C, the surface of the β-GaS:Mn plate is covered with a quasi-homogeneous array of nanowires with a length of about 1 μm and a thickness of (40–70) nm (Fig. 1c). At the temperature of 850 °C and much more intensively, the sublimation of gallium oxide takes place, and by condensation of the vapors, the compound of nanowires is formed on substrate as β-Ga_2O_3/GaS:Mn (Fig. 1 c, d). The steps of formation of β-Ga_2O_3 nanowires on the surface of GaSe plates subjected to thermal annealing (TT) at high temperatures in oxygen atmosphere is well described in the paper [22]. The mechanism of formation of β-Ga_2O_3:Mn nanowire assemblies on the surface of the β-Ga_2O_3 polycrystal is dominated by vapor–solid growth mechanism and can be explained considering the minimization of surface free energy, that facilitate directional growth. When the temperature of thermal annealing is increased up to 920 °C, the surface of the plates is covered with island regions of nano formation arrays on which fine wires with lengths of (5–7) μm and a thickness ranging from 38 nm to 78 nm are clearly visible (Fig. 1d).

3.2. X-ray diffraction (XRD)

Fig. 2a shows the XRD diffractogram of the GaS:Mn crystal. In the 2θ range of 20°–90°, five intense diffraction peaks are highlighted with intensity maxima centered at 2θ angles of: 23.08°, 34.78°, 46.97°, 73.33°, 88.23° and low intensity lines are at 50.65°, 59.62° and 80.63°. According to the PDF card-710009, these lines are identified as X-ray diffractions with a wavelength of $\lambda_{CuK\alpha} = 1.54060$ Å from planes with

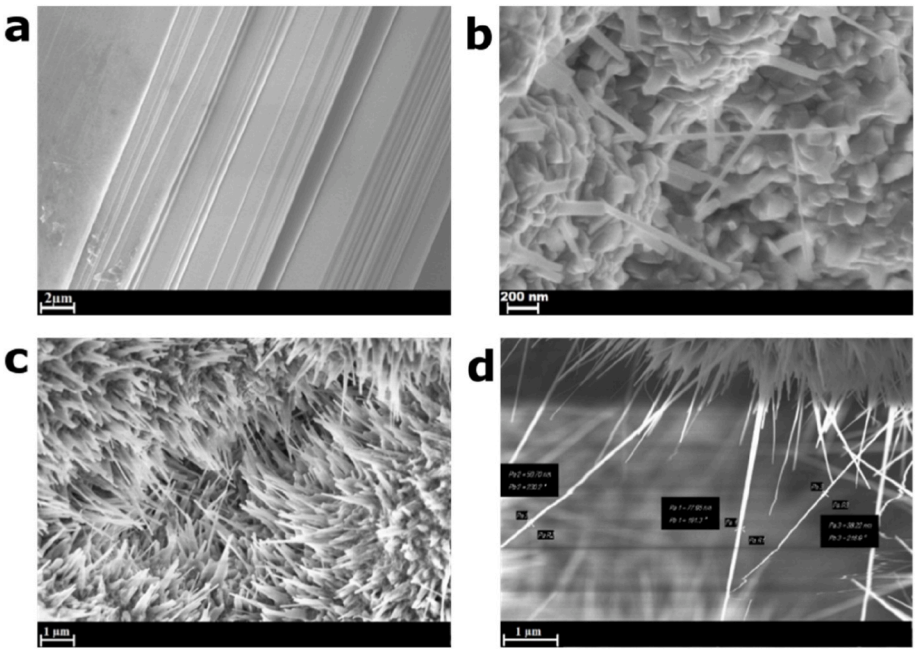


Fig. 1. SEM images of the cross-section of (**a**) single crystal GaS with 1.3 at.% Mn, (**b**) β-Ga_2O_3:Mn nano-formations obtained by thermal annealing in a water vapor atmosphere from single-crystal β-GaS doped with 1.3 at.% Mn at 850 °C for 6 h, (**c**) arrays of β-Ga_2O_3:Mn nanowires/nanosheets grown at 920 °C and (**d**) separated β-Ga_2O_3:Mn microwires.

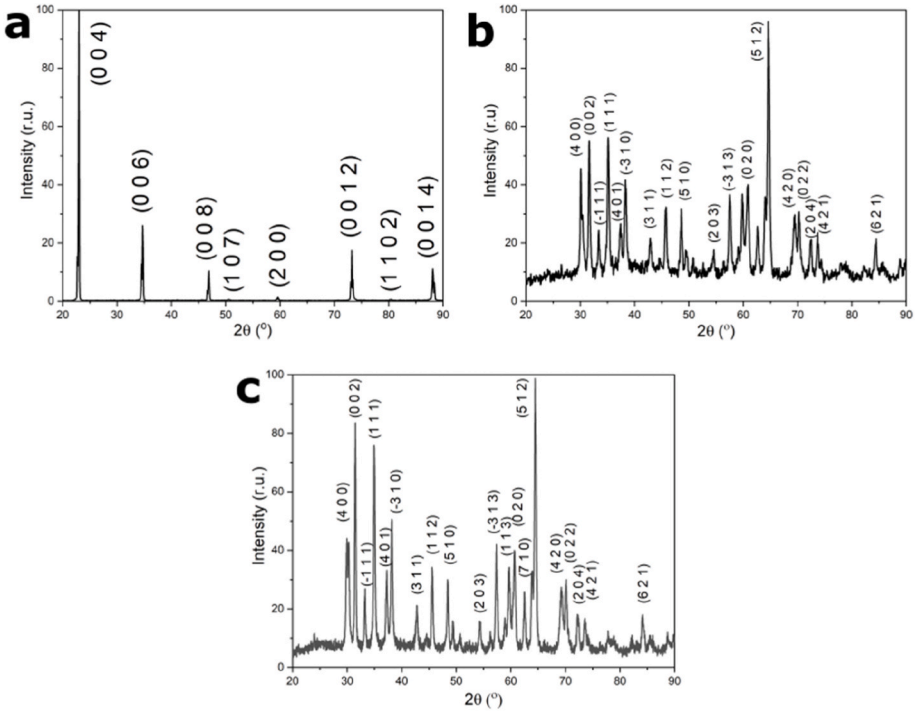


Fig. 2. XRD patterns of (**a**) GaS + 1.3 at.% Mn primary crystals, (**b**) β-Ga_2O_3:Mn obtained by thermal annealing at 850 °C for 6 h, (**c**) array of β-Ga_2O_3:Mn nanowires/nanosheets obtained at 920 °C.

Miller indices (0 0 4), (0 0 6), (0 0 8) and (4 0 0), (0 0 1 2), (0 0 1 4) and (1 0 7), (2 0 0), (1 0 1 2) respectively of the β-GaS hexagonal lattice with a = 3.585 Å and c = 15 492 Å.

The XRD patterns of the material obtained by thermal annealing in H_2O-enriched atmosphere for 6 h at the temperatures of 850 °C and 920 °C are shown in Fig. 2b and c, respectively. From the comparison of these three diagrams (Fig. 2 a, **b** and **c**), the absence of the diffraction lines of the primary material (GaS: 1.3 at% Mn) in Fig. 2b and c is clearly visible, indicating the complete oxidation of the GaS:Mn plate.

The absence of additional reflections in the range of 2θ diffraction angles from 20° to 90° draw a conclusion that the primary materials (GaS single crystals with 1.3 at% Mn and the β-Ga_2O_3:Mn layer) are monophasic and structurally homogeneous.

The sharp profile of the reflections in Fig. 2c compared to those in Fig. 2b can be used as a criterion for the high structural perfection of the β-Ga_2O_3 crystals.

According to the PDF card No 760573, the diffraction lines (XRD) indexed in Fig. 2b and **c** are identified as X-ray diffraction with the wavelength $\lambda_{CuK\alpha} = 1.54060$ Å from the crystallographic planes of the β-Ga_2O_3 phase with a monoclinic crystal lattice with the parameters a = 12.23 Å, b = 3.040 Å, c = 2.800 Å and β = 103.70°.

In the process of oxidation of the single crystal β-GaS:Mn at high temperatures, in addition to the formation of β-Ga_2O_3, a small amount of dopant Mn can form Mn_2O_3 compound. The formation of β-Ga_2O_3 and Mn_2O_3 phases by thermal annealing of β-GaS:Mn crystals is also favored by the correlation between the radii of Ga^{3+} (0.62 Å) and Mn^{3+} (0.64 Å) ions [19]. Y. Huang et al. [20] have shown that the presence of the mixture of β-Ga_2O_3/Mn_2O_3 phases in the XRD patterns is manifested by small shifts of the reflections with 2θ angles of 38.39 (−4 0 2) and 59.89° (1 1 3) (PDF card 760 573) towards smaller values of the 2θ angles at concentrations higher than 0.04 at.% of Mn in the compound. As can be seen from Fig. 2c, the reflections (0 0 4), (−4 0 2) and (1 1 3) in the studied material are found at 2θ angles of 38.18° and 59.66° and are shifted from the 2θ values observed by I. Goronovskii et al. [19] as 0.26°, 0.21° and 0.23°.

There is no doubt that the thermal annealing affects the crystallite growth mechanism, the crystallite shape and size. The average sizes of β-Ga_2O_3:Mn nanocrystallites in the substrate layer formed by high-temperature thermal annealing of GaS wafers doped with 1.3 at.% Mn were calculated using the Scherrer equation (1):

$$d = \frac{0.9\lambda}{\beta \cos\theta} \tag{1}$$

where d is the average size of the crystallite, θ is $2\theta/2$ where 2θ is the angle corresponding to the diffraction peak, λ is the wavelength of the X-rays and β is the full width at half maxima of the diffraction line. The parameter ε, which characterizes the micro-deformation of the crystallite is given by equation (2):

$$\varepsilon = \frac{\beta \cos\theta}{4} \tag{2}$$

To determine the parameters d and ε, the intensity peak at (0 0 2) with 2θ = 31.64° from Fig. 2b and the peak with 2θ = 31.48° from Fig. 2c were used. The full width at half maxima β of these peaks is equal to 0.29° and 0.25°, respectively.

The average crystallite sizes of β-Ga_2O_3 in the materials obtained at the annealing temperatures of 850 °C and 920 °C are equal to 28 nm and 33 nm, respectively. However, with the increase in the oxidation temperature of GaS:Mn crystals from 850 °C to 920 °C, a tendency to increase the size of β-Ga_2O_3:Mn nanocrystallites by ~15 % is observed, while the internal deformation factor (stress) ε has a decreasing tendency from $1.2{\cdot}10^{-3}$ to $1.05{\cdot}10^{-3}$. Such a tendency to increase the size of crystallites and decrease internal deformations in crystals and thin layers of semiconductors by thermal annealing has already been observed in previous works [21–23].

3.3. X-ray photoelectron spectroscopy (XPS)

The surface chemical composition of Mn-doped β-GaS slab subjected to thermal annealing at 850 °C for 6 h in a H_2O-enriched atmosphere were studied by XPS.

The maximum energy of the electrons excited in the material layer by X-rays of the wavelength $\lambda_{AlK\alpha} = 8.34$ Å does not exceed the photon energy of 1486 keV. The maximum thickness of the layer that can be penetrated by the XPS method upon excitation with the X-rays emitted by the Al anticathode, the penetration range R can be approximated using the Kanaya-Okayama empirical formula [24]:

$$R = \frac{0,0276}{\rho}\frac{A}{Z^{0.89}}E_0^n \tag{3}$$

where A is the atomic weight (g/mol), n is equal to ~1.35 for a primary energy $E_0 \leq 5$ keV, $E_0 = \frac{hc}{\lambda_{AlK\alpha}}$ – Roentgen energy of the electrons in (keV), Z is the number of atoms and ρ is the density (g/cm^3). For the compound β-Ga_2O_3, A_{Ga}≈69.7, $Z_{Ga} = 31$ and ρ = 5.863 g/cm^3 were chosen. From (3) the maximum thickness that can be penetrated is 26 Å.

The signal was averaged after three repeated scans in the energy region around 400 eV, while the high resolution spectrum was obtained by averaging 20 receivers of the 50 eV intervals. Fig. 3a shows the XPS spectrum scanned in the energy range of 0–1300 eV. In this spectrum, the signal for Ga 2p is clearly highlighted at ~1150 eV (Ga 2p 1/2) and 1123.0 eV (Ga 2p 3/2) and with the energy of 531 eV corresponding to the O/S oxygen in the Ga–O bond. At the same time, the generalized scan highlights the presence of oxygen and carbon on the surface of the sample. The manganese (Mn 2p) signal at 646 eV and a weak signal at ~180 eV are visible. This signal can be attributed to S 2p or Ga 3s. The presence of S atoms on the analyzed surface is possible since the base material subjected to thermal annealing is the GaS compound. The signals for Fe and Ca can be explained by the presence of these chemical elements in the sample support, while carbon can be caused by the adsorption of C–H compounds from the atmosphere. Fig. 3b shows the high resolution XPS spectrum in the 640–655 eV energy range. In this spectrum, the peak at 646 eV corresponding to the signal from Mn 2p is clearly highlighted.

3.4. Raman spectroscopy

Additional information on the structure and composition of the material obtained by thermal annealing of β-GaS:Mn nanosheets was obtained from the analysis of the Raman spectra. Fig. 4 shows the Raman spectra of β-GaS:Mn primary single crystals and β-Ga_2O_3:Mn material obtained by thermal annealing of β-GaS:Mn monocrystalline slabs in a H_2O vapor enriched atmosphere for 6 h at temperatures of 800 °C, 850 °C and 920 °C.

The Raman spectrum of GaS single crystals doped with 1.3 at.% of Mn in the range of wave numbers between 100 and 400 cm^{-1} contains three band modes with maxima centered at 189.13 cm^{-1}, 292.95 cm^{-1}, and 360.22 cm^{-1} (Fig. 4a). These bands correlate well with previous research [25], where they are identified as vibrational modes with symmetry A_{1g}^1 (189 cm^{-1}), A_{1g}^2 (360 cm^{-1}) and E_{2g}^1 (293 cm^{-1}) of the β-GaS hexagonal lattice. β-Ga_2O_3 with monoclinic structure belongs to the symmetry space group C_{2m}. For this group a total of 27 acoustic and optical vibrational modes are active in the center of the Brillouin zone: $\Gamma = 10A_g{+}4A_u{+}5B_g{+}8B_u$. 15 symmetric vibrational modes remain active: $\Gamma_R = 10A_g{+}5B_g$.

The Raman spectrum of the sample obtained by thermal annealing of monocrystalline GaS:Mn plates in air enriched with H_2O vapor at a temperature of 800 °C for 6 h is shown in Fig. 4b. In this spectrum there are four bands with maxima centered at the wavenumbers of 189.4 cm^{-1}, 234.9 cm^{-1}, 293.4 cm^{-1} and 360.4 cm^{-1}. The comparison of the spectrum in Fig. 4a and b shows the good match of the Raman spectrum of the primary material (GaS:Mn modes A_{1g}^1, A_{1g}^2 and E_{2g}^1) with the spectrum subjected to thermal annealing at 800 °C. At the same time, an additional band with a broad contour and maximum intensity centered at 233.9 cm^{-1} and three weakly pronounced plateaus at 390 cm^{-1}, 415 cm^{-1} and 473 cm^{-1} appear which are shown Fig. 4b. The band at 233.9 cm^{-1} and the plateaus at 390 cm^{-1} reported in the previous study [26] are identified as vibrational modes of the α-Ga_2S_3 Wurtzite lattice, while the features at 415 cm^{-1} and 473 cm^{-1} reported in the previous study [27] are interpreted as symmetric vibrational modes A_g (415 cm^{-1}) and B_g (475 cm^{-1}) of the bonds in the Ga_2O_6 octahedra in the monoclinic β-Ga_2O_3 lattice. The phase transformation mechanism of the GaS compound into Ga_2S_3 and further into Ga_2O_3 at the temperature of 800 °C can be described by the reaction [28]:

$$GaS + \frac{1}{4}O_2 = \frac{1}{3}Ga_2S_3 + \frac{1}{6}Ga_2O_3$$

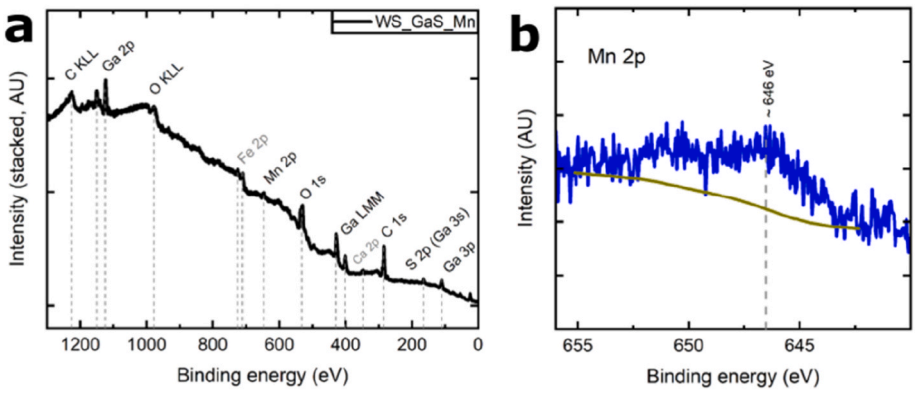


Fig. 3. (**a**) Overview of the XPS spectra of the β-Ga_2O_3:Mn sample: The overview spectra indicate that O, C, Ga, S and Mn are present at the sample surface. The indicated signals from Fe and Ca can be attributed to the sample holder. (**b**) High-resolution scan of the Mn 2p intensity.

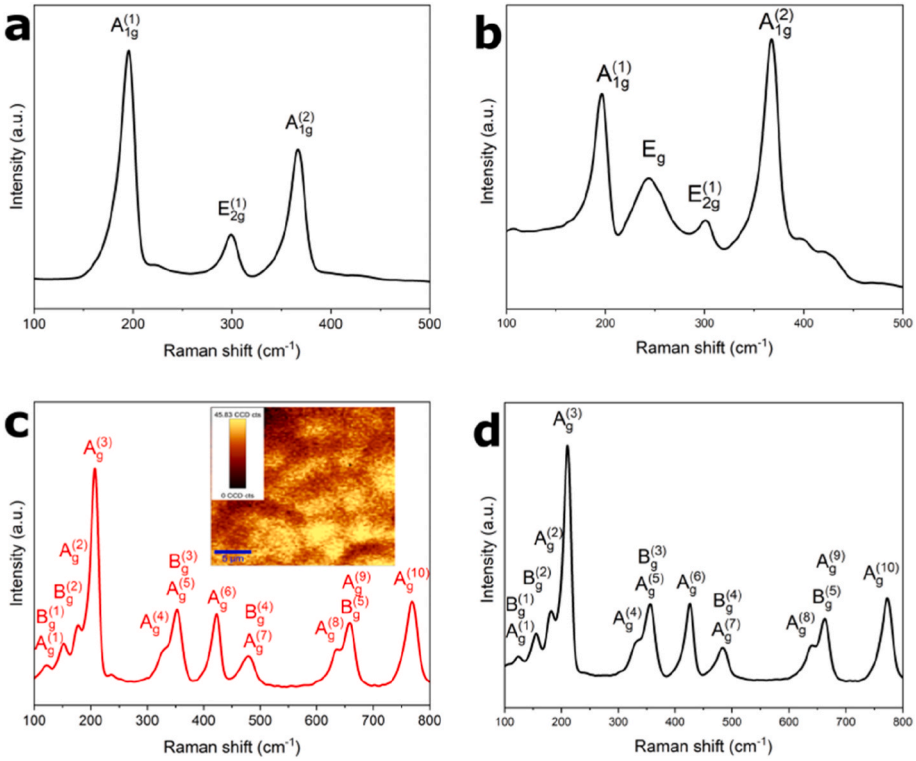


Fig. 4. Raman spectra of (**a**) primary GaS crystals with 1.3 at.% Mn and of the material obtained by thermal annealing of GaS:Mn single crystals in the H_2O vapor-enriched atmosphere at the temperature of (**b**) 800 °C; (**c**) 850 °C, (inset) filtered Raman image of GaS 1.3 at.% Mn after annealing at 850 °C for 6 h in terms of the mode A_g^{10} (767 cm^{-1}) corresponding to β-Ga_2O_3:Mn and (**d**) 920 °C.

The cardinal Raman spectrum changes, as the annealing temperature for β-GaS:Mn crystals is increased to 850 °C. In the range of wave numbers 100-800 cm^{-1}, three types of vibrational modes are clearly observed at low frequencies: B_g^1 (114 cm^{-1}), B_g^2 (145 cm^{-1}), A_g^2 (169 cm^{-1}), A_g^3 (199 cm^{-1}), mid-frequencies: A_g^4 (321 cm^{-1}), A_g^5, B_g^3 (345 cm^{-1}), A_g^6 (416 cm^{-1}), B_g^4 (473 cm^{-1}) and high frequencies: A_g^8 (627 cm^{-1}), B_g^5 A_g^9 (651 cm^{-1}), A_g^{10} (763 cm^{-1}). Increasing the annealing temperature to 920 °C does not change the structure of the Raman spectrum. A slight enhancement of the contours of the vibrational bands is observed (Fig. 4d). In the previous study [27], the low-frequency vibrational modes are interpreted as librations and translations of the chains of atoms in the monoclinic β-Ga_2O_3 network, the mid-frequency bands correspond to deformations in the Ga_2O_6 octahedra, while the high-frequency bands represent elongations and contractions in the GaO_4 tetrahedra. Fig. 4c (inset) shows the surface image mapping of the β-Ga_2O_3:Mn layer obtained by thermal annealing of the monocrystalline β-GaS:Mn slabs at the temperature of 850 °C for 6 h mapped from A_g^{10} (761 cm^{-1}). From this image, the micro-island structure of the surface of the gallium oxide (β-Ga_2O_3) layer can be clearly seen. The average size of the islands is ~3–5 μm. These inhomogeneities likely determine the intense light diffusion from the UV-VIS regions of these samples.

3.5. *Diffuse reflectance spectroscopy*

The spectral dependence of the diffuse reflection coefficient (Rd) from the surface of the sample obtained at a temperature of 800 °C contains two intervals to increase the Rd coefficient with the wavelengths of the incident radiation at 390–450 nm and 470–520 nm (Fig. 5a). The diffuse reflection coefficient Rd and the absorption

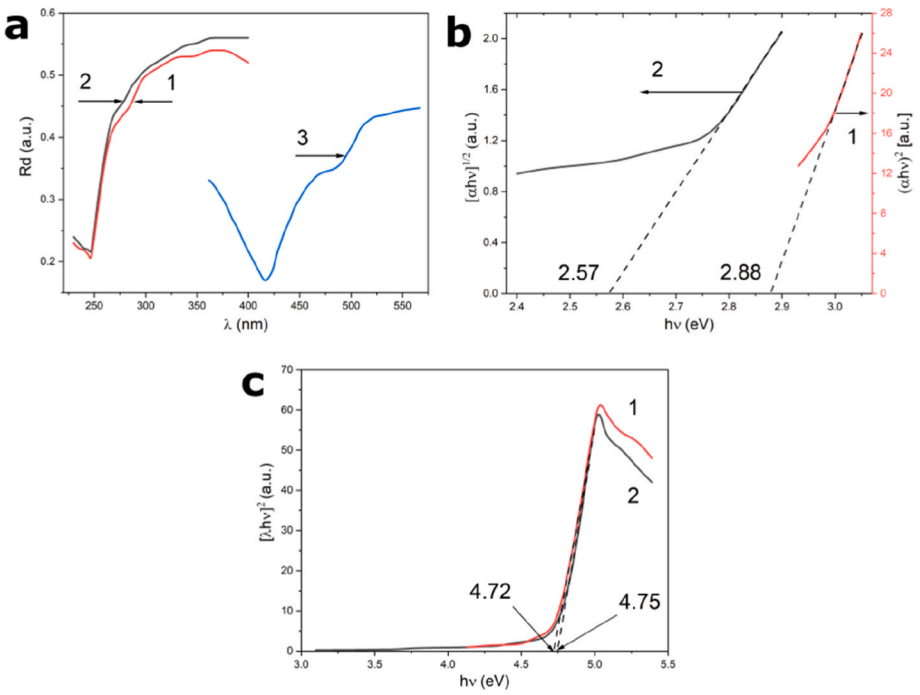


Fig. 5. (**a**) Diffuse reflectance spectra of the α-Ga_2S_3, GaS:Mn composite obtained at the temperature of 800 °C (3) and of the β-Ga_2O_3:Mn nanoformations obtained at 850 °C (1) and 920 °C (2). (**b**) Photon energy dependence of $(\alpha h\nu)^2$ (1) and $(\alpha h\nu)^{1/2}$ (2), (**c**) Absorbtion of radiation in the layer of β-Ga_2O_3:Mn nanoformations obtained at 850 °C (1) and 920 °C (2).

coefficient α are related by the Kubelka-Munk function [29]:

$$F(Rd) = \frac{(1 - Rd)^2}{2Rd} = \frac{\alpha}{s} \tag{4}$$

where s is the wavelength-independent scattering factor for material with grains larger than the wavelength of the incident radiation. The absorption of light in semiconductors by momentum-conserving electronic transitions is described by the formula [30]:

$$\alpha(h\nu) = (h\nu - Eg)^n \tag{5}$$

where E_g is the forbidden bandwidth and $n = 2$ for indirect transitions, while $n = 1/2$ for direct transitions.

As can be seen from Fig. 5b, in the wavelength range of 390–450 nm corresponding to 3.20–2.76 eV, the dependence of the photon energy absorption coefficient corresponds to direct optical transitions with E_{g0} = 2.88 eV, while in the energy range 2.60-2.38 eV indirect optical transitions are achieved with E_{gi} = 2.57 eV. These values correlate well with the width of the direct band gap in α-Ga_2S_3 crystals and with the width of the indirect band gap in GaS, respectively. The direct band gap of the cubic α-Ga_2S_3 phase has been previously determined to be in the energy range of 2.7–3.0 eV [31,32]. The indirect band gap in GaS lamellar crystals at 300 K is equal to 2.53 eV [33]. Fig. 5c shows the spectral dependence of the absorption coefficient as a function of the photon energy of the material layer obtained by thermal annealing in the atmosphere enriched with H_2O vapors at the temperature of 850 °C (curve 1) and 920 °C (curve 2) of the plates of GaS doped with 1.3 % of Mn. The edge of the absorption band of these materials is well described by formula (5) with n = 1/2 and corresponds to direct optical transitions with E_g = 4.72 eV and 4.75 eV, respectively. The band gap in undoped β-Ga_2O_3 crystals is 4.85 eV [34].

Doping the β-Ga_2O_3 compound with S, Zn, In, Nb or Mn leads to a narrowing of the band gap, E_g is in the range of 4.0–4.9 eV [35–38]. For thin layers of β-Ga_2O_3 on a sapphire substrate the band gap is 5.06 eV. Doping them with 2 % of Mn reduces the band gap to 4.46 eV [20].

3.6. Photoluminescence (PL)

The PL of the material layer obtained by thermal annealing of monocrystalline GaS plates doped with 1.3 at% of Mn in air enriched with H_2O vapor was studied at the temperature of 80 K. The PL spectra of the material obtained by thermal annealing at the temperature of 800 °C under excitation with laser radiation at λ = 405 nm are presented in Fig. 6, curve 1. As can be seen, the PL spectrum has a complex structure in which the red band with a maximum centered at ~692 nm (1792 eV) is dominant in terms of intensity. A medium intensity band with a maximum at 516 nm (2.403 eV) and a plateau with an edge at ~590 nm (2.10 eV) are also highlighted. The XRD pattern and Raman spectrum of this sample shows that this material is composed of GaS and

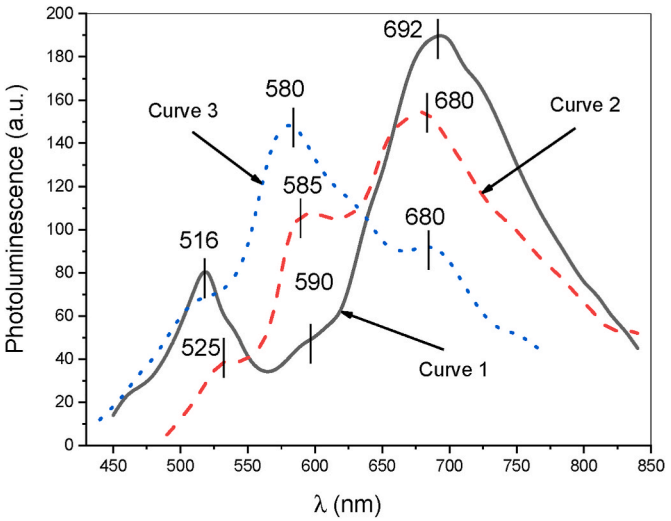


Fig. 6. Photoluminescence of the surface of the material obtained by thermal annealing of GaS:Mn single crystals in air enriched with H_2O vapors for 6 h at the temperature 800 °C (curve1); 850 °C (curve 2) and 920 °C (curve 3).

Ga_2S_3 crystallites.

The PL spectrum of GaS crystals at 80 K is well studied and contains a band of low intensity in the absorption band edge region with a maximum at 483 nm and another with dominant intensity in the near-IR region with a maximum at ~1000 nm [39,40]. The photoluminescence of Mn-doped GaS crystals has been previously investigated in papers [39,41]. In the PL spectrum of Mn doped GaS crystals, the band with maximum intensity at 619 nm (2002 eV) predominates. The PL spectrum of α-Ga_2S_3 crystals contains two bands with maxima centered at 420 nm (2.93 eV) and 635 nm (1.95 eV) [42]. This shows that the PL bands of α-Ga_2S_3, GaS, GaS:Mn crystals do not affect the spectral structure of the investigated sample set. The low-temperature photoluminescence of Mn-doped Ga_2S_3 single crystals has been extensively studied by J. S. Lee et al. [43]. In this work, based on the measurements of optical spectra (PL, TSC – thermally stimulated current and PICTS – thermally stimulated photoinduced current), the energy level diagrams of the Mn^{+2} ion in α-Ga_2S_3 crystals were constructed. Based on this diagram the PL bands with intensity maxima at 692 nm (1.80 eV), 516 nm (2.40 eV) and the plateau at 585 nm (2.12 eV) can be interpreted as radiative electron transitions in the Mn^{2+} ion $^4T_1(^4G)\rightarrow A_2$, $^4T_1(^4G)\rightarrow {}^6A_1(^6S)$ and $^4T_1(^4G)\rightarrow A_1$, respectively.

The PL spectrum of β-Ga_2S_3 crystals contains an intense band with a maximum centered at 425 nm (2.95 eV). For nanostructured β-Ga_2O_3 this band is located at 470 nm (2.64 eV) [13,14]. In the PL spectra of β-Ga_2O_3:Mn nanoformations obtained at the temperature of 850 °C (Fig. 6 curve 2) and 920 °C (Fig. 6 curve 3), the maximum of the band is centered at 680 nm (1.82 eV), 585 nm (2.12 eV) and 580 nm (2.14 eV), respectively. At the same time, in these spectra, the peculiarities with drops at 525 nm (2.36 eV), 580 nm (2.14 eV), and 680 nm (1.80 eV) are highlighted. Considering the good structural analogy between the Ga_2S_3 and Ga_2O_3 compounds, the PL bands of the β-Ga_2O_3:Mn layers in Fig. 6, curves 2 and 3 can be interpreted based on the diagram of electronic transitions $^4T_1(G)\rightarrow {}^6A_1(^6S)$, $^4T_1(G)\rightarrow A_1$ and $^4T_1(G)\rightarrow A_2$ in the Mn^{2+} ion.

We note that the PL spectrum of the β-Ga_2O_3:Mn nanowires studied in the paper [44] contains a broad band covering the wavelength range of 400–680 nm, with a maximum at 520 nm.

4. Conclusions

By thermal annealing of single-crystalline β-GaS plates doped with 1.3 at.% Mn in an atmosphere enriched with H_2O vapor at a temperature of 800 °C for 6 h, their surface is covered with a layer of a composite consisting of crystallites of Ga_2S_3:Mn and GaS:Mn with a direct band gap of 2.88 eV and an indirect band gap of 2.55 eV with a PL spectrum determined by electronic transitions in the Mn^{2+} ion. Upon increasing the thermal annealing temperature to 850 °C and 920 °C, the surface of the β-GaS:Mn samples is covered with a layer consisting of β-Ga_2O_3:Mn nanowires/nanosheets with band gaps of 4.72 eV and of 4.75 eV, respectively. The photoluminescence was determined by electronic transitions in the Mn^{2+} ion.

Funding

This research was funded by National Agency for Research and Development, grant number 20.80009.7007.05".

CRediT authorship contribution statement

Veaceslav Sprincean: Writing – original draft, Validation, Investigation, Funding acquisition. **Haoyi Qiu:** Visualization, Methodology, Investigation, Formal analysis. **Oleg Lupan:** Writing – original draft, Validation, Supervision, Investigation, Data curation, Conceptualization. **Tim Tjardts:** Visualization, Software, Investigation. **Deik Petersen:** Writing – review & editing, Methodology, Investigation. **Salih Veziroglu:** Writing – review & editing, Supervision, Software, Resources, Data curation. **Rainer Adelung:** Writing – review & editing, Funding acquisition, Formal analysis. **Mihail Caraman:** Writing – review & editing, Validation, Supervision, Conceptualization.

Declaration of competing interest

The authors declare that they have no known competing financial interests or personal relationships that could have appeared to influence the work reported in this paper.

Data availability

No data was used for the research described in the article.

Acknowledgments

VS and MC gratefully acknowledge the support provided by the National Agency for Research and Development and the Moldova State University through grant number 20.80009.7007.05. We acknowledge funding from the - SulfurSilicon Batteries (SuSiBaBy) Project from the EUSH and EFRE in SH (LPW-E/3.January 1, 1801). The German Research Foundation (DFG- Deutsche For-schungsgemeinschaft) provided additional support through various schemes, including Project-ID 434434223-SFB 1461, Project-ID 286471992-SFB 1261 project A2, GRK 2154 project P4 and AD 183/16-1.

References

[1] J.Y. Tsao, S. Chowdhury, M.A. Hollis, D. Jena, N.M. Johnson, K.A. Jones, R. J. Kaplar, S. Rajan, C.G. Van de Walle, E. Bellotti, C.L. Chua, R. Collazo, M. E. Coltrin, J.A. Cooper, K.R. Evans, S. Graham, T.A. Grotjohn, E.R. Heller, M. Higashiwaki, M.S. Islam, P.W. Juodawlkis, M.A. Khan, A.D. Koehler, J.H. Leach, U.K. Mishra, R.J. Nemanich, R.C.N. Pilawa-Podgurski, J.B. Shealy, Z. Sitar, M. J. Tadjer, A.F. Witulski, M. Wraback, J.A. Simmons, Ultrawide-bandgap semiconductors: research opportunities and challenges, Adv. Electron. Mater. 4 (2018), https://doi.org/10.1002/aelm.201600501.

[2] J. Zhang, J. Shi, D.-C. Qi, L. Chen, K.H.L. Zhang, Recent progress on the electronic structure, defect, and doping properties of Ga 2 O 3, Apl. Mater. 8 (2020), 020906, https://doi.org/10.1063/1.5142999.

[3] T.F. Weng, M.S. Ho, C. Sivakumar, B. Balraj, P.F. Chung, VLS growth of pure and Au decorated β-Ga2O3 nanowires for room temperature CO gas sensor and resistive memory applications, Appl. Surf. Sci. 533 (2020), https://doi.org/10.1016/j.apsusc.2020.147476.

[4] M. Baldini, Z. Galazka, G. Wagner, Recent progress in the growth of β-Ga2O3 for power electronics applications, Mater. Sci. Semicond. Process. 78 (2018) 132–146, https://doi.org/10.1016/j.mssp.2017.10.040.

[5] S.J. Pearton, J. Yang, P.H. Cary, F. Ren, J. Kim, M.J. Tadjer, M.A. Mastro, A review of Ga2O3 materials, processing, and devices, Appl. Phys. Rev. 5 (2018), https://doi.org/10.1063/1.5006941.

[6] S. Elafandi, Z. Ahmadi, N. Azam, M. Mahjouri-Samani, Gas-phase formation of highly luminescent 2D GaSe nanoparticle ensembles in a nonequilibrium laser ablation process, Nanomaterials 10 (2020), https://doi.org/10.3390/nano10050908.

[7] G. Chen, L. Zhang, L. Li, F. Cheng, X. Fu, J. Li, R. Pan, W. Cao, A.S. Chan, G. N. Panin, J. Wan, H. Zhang, C. Liu, GaSe layered nanorods formed by liquid phase exfoliation for resistive switching memory applications, J. Alloys Compd. (2020) 823, https://doi.org/10.1016/j.jallcom.2020.153697.

[8] E. Chikoidze, T. Tchelidze, C. Sartel, Z. Chi, R. Kabouche, I. Madaci, C. Rubio, H. Mohamed, V. Sallet, F. Medjdoub, A. Perez-Tomas, Y. Dumont, Ultra-high critical electric field of 13.2 MV/cm for Zn-doped p-type β-Ga2O3, Mater. Today Phys. 15 (2020), https://doi.org/10.1016/j.mtphys.2020.100263.

[9] M. Zervos, A. Othonos, V. Gianneta, A. Travlos, A.G. Nassiopoulou, Sn doped β-Ga2O3 and β-Ga2S3 nanowires with red emission for solar energy spectral shifting, J. Appl. Phys. 118 (2015), https://doi.org/10.1063/1.4935633.

[10] M. Ogita, K. Higo, Y. Nakanishi, Y. Hatanaka, Ga2O3 thin film for oxygen sensor at high temperature, Appl. Surf. Sci. 175–176 (2001) 721–725, https://doi.org/10.1016/S0169-4332(01)00080-0.

[11] R. Ito, M. Akatsuka, A. Ozawa, Y. Kato, Y. Kawaguchi, M. Yamamoto, T. Tanabe, T. Yoshida, Photocatalytic activity of Ga 2 O 3 supported on Al 2 O 3 for water splitting and CO 2 reduction, ACS Omega 4 (2019) 5451–5458, https://doi.org/10.1021/acsomega.9b00048.

[12] B. Alhalaili, R. Vidu, M.S. Islam, The growth of Ga2O3 nanowires on silicon for ultraviolet photodetector, Sensors (2019) 19, https://doi.org/10.3390/s19235301.

[13] J. Jiang, J. Zhang, Z. Song, Influence of Zn doping on the morphology and luminescence of Ga2O3 low-dimensional nanostructures, J. Lumin. 221 (2020), https://doi.org/10.1016/j.jlumin.2020.117048.

[14] F. Alema, B. Hertog, O. Ledyaev, D. Volovik, G. Thoma, R. Miller, A. Osinsky, P. Mukhopadhyay, S. Bakhshi, H. Ali, W.V. Schoenfeld, Solar blind photodetector

based on epitaxial zinc doped Ga2O3 thin film, Physica Status Solidi (A) Appli. Mater. Sci. (2017) 214, https://doi.org/10.1002/pssa.201600688.
[15] G. Gundiah, A. Govindaraj, C.N.R. Rao, Nanowires, nanobelts and related nanostructures of Ga2O3, Chem. Phys. Lett. 351 (2002) 189–194, https://doi.org/10.1016/S0009-2614(01)01372-0.
[16] S. Kumar, S. Dhara, R. Agarwal, R. Singh, Study of photoconduction properties of CVD grown β-Ga2O3 nanowires, J. Alloys Compd. 683 (2016) 143–148, https://doi.org/10.1016/j.jallcom.2016.05.079.
[17] B. Zhao, F. Wang, H. Chen, Y. Wang, M. Jiang, X. Fang, D. Zhao, Solar-Blind avalanche photodetector based on single ZnO-Ga2O3 core-shell microwire, Nano Lett. 15 (2015) 3988–3993, https://doi.org/10.1021/acs.nanolett.5b00906.
[18] X. Wang, R. Quhe, Y. Zhi, Z. Liu, Y. Huang, X. Dai, Y. Tang, Z. Wu, W. Tang, The electronic structure and magnetic property of the Mn doped β-Ga2O3, Superlattice. Microst. 125 (2019) 330–337, https://doi.org/10.1016/j.spmi.2018.12.001.
[19] I. Goronovskii, Y.P. Nazarenko, E. Nekryach, Concise Handbook of Chemistry, 1987.
[20] Y. Huang, Z. Liu, J. Wang, Y. Zhi, D. Guo, X. Wang, X. Wang, Z. Chen, P. Li, W. Tang, The effect of Mn dopant on structural and optoelectronic properties of γ-Ga 2 O 3 thin film photodetectors, ECS J. Solid State Sci. Technol. 9 (2020), 055010, https://doi.org/10.1149/2162-8777/ab9ab3.
[21] Z. Chen, X. Wang, K. Saito, T. Tanaka, M. Nishio, Q. Guo, The impact of growth temperature on the structural and optical properties of catalyst-Free β-Ga2O3 nanostructures, Mater. Res. Express 3 (2016), https://doi.org/10.1088/2053-1591/3/2/025003.
[22] E. Filippo, M. Siciliano, A. Genga, G. Micocci, A. Tepore, T. Siciliano, Single crystalline β-Ga2O3 nanowires synthesized by thermal oxidation of GaSe layer, Mater. Res. Bull. 48 (2013) 1741–1744, https://doi.org/10.1016/j.materresbull.2012.08.083.
[23] S.Y. Lee, H.C. Kang, Synthesis and characterization of β-Ga2O3 nanowires on amorphous substrates using radio-frequency powder sputtering, J. Cryst. Growth 412 (2015) 25–30, https://doi.org/10.1016/j.jcrysgro.2014.11.030.
[24] S. Okayama, K. Kanaya, Penetration and energy-loss theory of electrons in solid targets, J. Phys. D Appl. Phys. 5 (1972) 43.
[25] C. Jastrzebski, K. Olkowska, D.J. Jastrzebski, M. Wierzbicki, W. Gebicki, S. Podsiadlo, Raman scattering studies on very thin layers of gallium sulfide (GaS) as a function of sample thickness and temperature, J. Phys. Condens. Matter 31 (2019), https://doi.org/10.1088/1361-648X/aaf53b.
[26] C.H. Ho, M.H. Lin, Y.P. Wang, Y.S. Huang, Synthesis of In2S3 and Ga2S3 crystals for oxygen sensing and UV photodetection, Sensor Actuator Phys. 245 (2016) 119–126, https://doi.org/10.1016/j.sna.2016.05.003.
[27] D. Dohy, G. Lucazeau, Valence force field and Raman spectra of β Ga2O3, J. Mol. Struct. 79 (1982) 419–422, https://doi.org/10.1016/0022-2860(82)85094-1.
[28] O.A. Balitskii, V.P. Savchyn, P.V. Savchyn, Thermal oxidation of indium and gallium sulphides, Phys. B Condens. Matter 355 (2005) 365–369, https://doi.org/10.1016/j.physb.2004.11.033.
[29] S.I. Boldish, W.B. White, Optical band gaps of selected ternary sulfide minerals, Am. Mineral. 83 (1998) 865–871, https://doi.org/10.2138/am-1998-7-818.
[30] J.I. Pankove, Optical Processes in Semiconductors, 1971.
[31] K.A. Kokh, Z.M. Huang, J.G. Huang, Y.Q. Gao, B. Uralbekov, J. Panomarev, I. N. Lapin, V.A. Svetlichnyi, G.V. Lanskii, Y.M. Andreev, Study of Ga2S3 crystals grown from melt and PbCl2 flux, Mater. Res. Bull. 84 (2016) 462–467, https://doi.org/10.1016/j.materresbull.2016.08.046.
[32] H.F. Liu, K.K.A. Antwi, N.L. Yakovlev, H.R. Tan, L.T. Ong, S.J. Chua, D.Z. Chi, Synthesis and phase evolutions in layered structure of Ga2S 3 semiconductor thin films on epiready GaAs (111) substrates, ACS Appl. Mater. Interfaces 6 (2014) 3501–3507, https://doi.org/10.1021/am4056535.
[33] M. Isik, E. Tugay, N. Gasanly, Optical properties of GaS crystals: combined study of temperature-dependent band gap energy and oscillator parameters, Indian J. Pure Appl. Phys. 55 (2017) 583–588.
[34] Z. Galazka, S. Ganschow, K. Irmscher, D. Klimm, M. Albrecht, R. Schewski, M. Pietsch, T. Schulz, A. Dittmar, A. Kwasniewski, R. Grueneberg, S. Bin Anooz, A. Popp, U. Juda, I.M. Hanke, T. Schroeder, M. Bickermann, Bulk single crystals of β-Ga2O3 and Ga-based spinels as ultra-wide bandgap transparent semiconducting oxides, Prog. Cryst. Growth Char. Mater. 67 (2021), https://doi.org/10.1016/j.pcrysgrow.2020.100511.
[35] J.X. Chen, X.X. Li, J.J. Tao, H.Y. Cui, W. Huang, Z.G. Ji, Q.L. Sai, C.T. Xia, H.L. Lu, D.W. Zhang, Fabrication of a Nb-doped β-Ga2O3 nanobelt field-effect transistor and its low-temperature behavior, ACS Appl. Mater. Interfaces 12 (2020) 8437–8445, https://doi.org/10.1021/acsami.9b20499.
[36] M. Fang, W. Zhao, F. Li, D. Zhu, S. Han, W. Xu, W. Liu, P. Cao, M. Fang, Y. Lu, Fast response solar-blind photodetector with a quasi-zener tunneling effect based on amorphous in-doped Ga2O3 thin films, Sensors (2020) 20, https://doi.org/10.3390/s20010129.
[37] F. Du, D. Yang, Y. Sun, Y. Jiao, F. Teng, H. Fan, Electrospun Zn-doped Ga2O3 nanofibers and their application in photodegrading rhodamine B dye, Ceram. Int. 47 (2021) 4963–4971, https://doi.org/10.1016/j.ceramint.2020.10.072.
[38] D. Guo, Z. Wu, Y. An, X. Li, X. Guo, X. Chu, C. Sun, M. Lei, L. Li, L. Cao, P. Li, W. Tang, Room temperature ferromagnetism in (Ga 1−x Mn x) 2 O 3 epitaxial thin films, J. Mater. Chem. C 3 (2015) 1830–1834, https://doi.org/10.1039/C4TC02833C.
[39] S. Shigetomi, T. Ikari, Radiative transitions of layered semiconductor GaS doped with P, J. Lumin. 118 (2006) 106–110, https://doi.org/10.1016/j.jlumin.2005.08.002.
[40] S. Shigetomi, T. Ikari, Radiative centers in layered semiconductor GaS doped with Zn, J. Lumin. 113 (2005) 137–142, https://doi.org/10.1016/j.jlumin.2004.09.116.
[41] S. Shigetomi, K. Sakai, T. Ikari, Photoluminescence of layered semiconductor GaS doped with Mn, Physica Status Solidi (B) Basic Res. 241 (2004) 2607–2612, https://doi.org/10.1002/pssb.200402044.
[42] T. Ahamad, S.M. Alshehri, Green synthesis and characterization of gallium(III) sulphide (α-Ga_2S_3) nanoparicles at room temperature, Nano Hybrids 6 (2014) 37–46. https://doi.org/10.4028/www.scientific.net/nh.6.37.
[43] J.S. Lee, Y.H. Won, H.N. Kim, C.D. Kim, W.T. Kim, Photoluminescence of Ga2S3 and Ga2S3: Mn single crystals, Solid State Commun. 97 (1996) 1101–1104, https://doi.org/10.1016/0038-1098(95)00728-8.
[44] Y.P. Song, P.W. Wang, X.Y. Xu, Z. Wang, G.H. Li, D.P. Yu, Magnetism and photoluminescence in manganese-gallium oxide nanowires with monoclinic and spinel structures, Phys. E Low-dimens. Syst. Nanostruct. 31 (2006) 67–71, https://doi.org/10.1016/j.physe.2005.09.003.